Robust repetitive control of grid-connected DC-AC converters[1]

Qing-Chang Zhong, Tim Green, Jun Liang, George Weiss
Dept. of Electrical & Electronic Engineering
Imperial College of Science, Technology and Medicine
Exhibition Rd., London, SW7 2BT, UK

Abstract

This paper proposes a possible circuit topology and voltage controller design for connecting a DC-AC converter to the power grid. This converter is meant to operate in conjunction with a small power generating unit. The design of the output voltage controller is based on H^∞ and repetitive control. This leads to a very low harmonic distortion of the output voltage, even in the presence of nonlinear loads and/or a distorted grid voltage (The complete controller has also other components besides the output voltage controller, which will be discussed elsewhere). The output voltage controller contains an infinite-dimensional internal model, which enables it to reject all periodic disturbances which have the same period as the grid voltage, and whose highest frequency components are up to approximately 1.5kHz.

Index Terms: Repetitive control, DC-AC power converter, H^∞ control

1 Introduction

For various reasons, there is today a proliferation of small power generating units which are connected to the power grid at the low-voltage end. Some of these units use synchronous generators, but most use DC or variable frequency generators coupled with electronic power converters. For example, wind-turbines are most effective if free to generate at variable frequency, so they need AC (variable frequency) to DC and then to AC (50Hz) conversion [1]; small gas turbine-driven generators operate at high frequencies and so they also require AC-DC-AC conversion [2]; photo-voltaic arrays require DC-AC conversion [3]. The distribution network has relatively high supply impedances and distortion of both voltage and current waveforms are prevalent because of the existence of many non-linear loads (e.g. rectifiers, arc furnace etc.). The DC-AC power converters consist of semiconductor switching elements and passive components for filtering or short-term energy storage.

The power converters must track sinusoidal voltage references subject to non-sinusoidal current disturbances from rectifier or other nonlinear loads and a possibly distorted

grid voltage. The converters are advantageous here because they offer control possibilities not present in conventional generators. In principle, the instantaneous output of the power converter can be controlled to ensure that, despite distortion of the current in the network by some customers, other customers can receive an undistorted supply. Repetitive control [4, 5, 6, 7] offers a much better alternative for voltage tracking, as it can deal with a very large number of harmonics simultaneously, and even with several disturbances at different frequencies.

In this paper, we propose a circuit topology for connecting a DC-AC converter to the grid and we propose a certain design for the output voltage controller based on repetitive control, which leads to a very low harmonic distortion of the generated voltage, even in the presence of nonlinear loads. The main idea in the topology is that we create a "local grid" which is separated from the external grid by an inductor. The consumers connected to this local grid are called local consumers and the converter is connected to the local grid. This separation enables us to control the voltage of the local grid with high precision, even if the local consumers are highly nonlinear.

The voltage on the three phases of the local grid must track given sinusoidal reference signals. Assuming that the tracking is accurate, the amount of active and reactive power generated depends on the amplitudes and phases of these reference signals, which must be carefully synchronized with the grid voltages (without being equal to them). For this reason, the reference signals must be generated, taking into account voltage and current constraints, by another controller, called "power controller". This will be discussed elsewhere. In this paper, the reference signals are considered to be given and we only solve the tracking problem.

2 System description

The three phase power system consists of the converter (including the IGBT bridge and LC filters), the local consumers, the separating inductor and the (external) power grid. We regard this system as three independent single-phase systems, even though this assumption may be wrong, with coupling between the phases present in some consumers. The electrical diagram of one single-phase system,

which is our plant to be controlled, is shown in Figure 1. The inductors are modelled, taking into account their high frequency behavior, as an ideal inductor in parallel with a resistor and then in series with another resistor. The current source i_d models the harmonics caused by nonlinear loads and/or disturbances. Our control objective is to maintain the local grid voltage V_{out} as close as possible to the given reference voltage V_{ref}. The two switches S_c and S_g appearing in Figure 1 are needed in the start-up and shut-down procedures of the converter. In this paper, the switches are considered to be closed. The parameters of the system are shown in Table 1. The switching frequency of the IGBT bridge is 10kHz. The PWM block is designed such that for $|u(t)| < 425$V, the local average of the bridge output voltage u_f equals u.

We take the state variables as the currents of the three inductors and the voltage of the capacitor ($V_c = V_{out}$, since S_c is closed). The external input variables are i_d, V_g and V_{ref} and the control input is u. Thus,

$$x = \begin{bmatrix} i_1 \\ i_2 \\ i_3 \\ V_c \end{bmatrix}, \qquad \left[\begin{array}{c} w \\ \hline u \end{array} \right] \doteq \begin{bmatrix} i_d \\ V_g \\ V_{ref} \\ \hline u \end{bmatrix}.$$

The state equation of the plant is

$$\dot{x} = Ax + \begin{bmatrix} B_1 & B_2 \end{bmatrix} \begin{bmatrix} w \\ u \end{bmatrix}, \qquad (1)$$

where

$$A = \begin{bmatrix} -\frac{R_f r_f}{(R_f+r_f)L_f} & 0 & 0 & -\frac{r_f}{(R_f+r_f)L_f} \\ 0 & -\frac{R_g r_g}{(R_g+r_g)L_g} & 0 & -\frac{r_g}{(R_g+r_g)L_g} \\ 0 & 0 & -\frac{Rr}{(R+r)L} & \frac{r}{(R+r)L} \\ \frac{r_f}{(R_f+r_f)C} & \frac{r_g}{(R_g+r_g)C} & -\frac{r}{(R+r)C} & -(\frac{1}{R+r} + \frac{1}{R_f+r_f} + \frac{1}{R_g+r_g})\frac{1}{C} \end{bmatrix},$$

$$\begin{bmatrix} B_1 & B_2 \end{bmatrix} = \left[\begin{array}{ccc|c} 0 & 0 & 0 & \frac{r_f}{(R_f+r_f)L_f} \\ 0 & \frac{r_g}{(R_g+r_g)L_g} & 0 & 0 \\ 0 & 0 & 0 & 0 \\ -\frac{1}{C} & \frac{1}{(R_g+r_g)C} & 0 & \frac{1}{(R_f+r_f)C} \end{array} \right].$$

The output signals from the plant are the tracking error $e = V_{ref} - V_c$ and the current i_c, so that $y = \begin{bmatrix} e & i_c \end{bmatrix}^T$. The output equations are

$$y = \begin{bmatrix} C_1 \\ C_2 \end{bmatrix} x + \begin{bmatrix} D_{11} & D_{12} \\ D_{21} & D_{22} \end{bmatrix} \begin{bmatrix} w \\ u \end{bmatrix},$$

where

$$\begin{bmatrix} C_1 \\ C_2 \end{bmatrix} = \left[\begin{array}{cccc} 0 & 0 & 0 & -1 \\ \hline 0 & -\frac{r_g}{R_g+r_g} & \frac{r}{R+r} & \frac{1}{R+r} + \frac{1}{R_g+r_g} \end{array} \right],$$

$$\begin{bmatrix} D_{11} & D_{12} \\ D_{21} & D_{22} \end{bmatrix} = \left[\begin{array}{ccc|c} 0 & 0 & 1 & 0 \\ \hline 1 & -\frac{1}{R_g+r_g} & 0 & 0 \end{array} \right].$$

The corresponding transfer function is

$$\mathbf{P}(s) = \left[\begin{array}{c|cc} A & B_1 & B_2 \\ \hline C_1 & D_{11} & D_{12} \\ C_2 & D_{21} & D_{22} \end{array} \right],$$

where we have used the compact notation now standard in control theory, see for example [8, 9].

3 Controller design

We will follow the H^∞ control-based design procedure for repetitive controllers proposed in [4], which uses additional measurement information from the plant. The block diagram of the control system is shown in Figure 2. The three external signals (the components of w) are assumed to be periodic, with a fundamental frequency of 50 Hz. The controller consists of an internal model and a stabilizing compensator. The internal model has an infinite sequence of pairs of conjugate poles of which about the first 30 are very close to the imaginary axis, around integer multiples of $2\pi \cdot 50i$, and the later ones are further to the left. The stabilizing compensator assures the exponential stability of the entire system. The error will then converge to a small steady-state error, see [4] for details.

As in [4], the internal model is obtained from a low-pass filter with transfer function

$$W(s) = \frac{\omega_c}{s + \omega_c}$$

with $\omega_c = 10000$ rad/sec, cascaded with a delay element with transfer function $e^{-\tau_d s}$, where τ_d is slightly less than the fundamental period $\tau = 20$msec:

$$\tau_d = \tau - \frac{1}{\omega_c} = 19.9 \text{ msec}.$$

After closing a positive unity feedback around this cascade connection, we obtain the internal model, as can be seen in Fig. 2. The choice of ω_c is based on a compromise: for ω_c too low, only few poles of the internal model will be close to the imaginary axis, leading to poor tracking and disturbance rejection at higher frequencies. For ω_c too high, the system is difficult to stabilize (a stabilizing $\mathbf{C}$ may not exist, or it may need high bandwidth).

According to [4], the closed-loop system in Fig. 2 is exponentially stable if the finite-dimensional closed-loop system from Fig. 3 is stable and its transfer function from a to b, denoted $\mathbf{T}_{ba}$, satisfies $\|\mathbf{T}_{ba}\|_\infty < 1$. Thus, we have to design $\mathbf{C}$ such that the above two conditions are satisfied. Moreover, we want to minimize $\frac{\gamma_0}{1-\gamma}$ while keeping $\gamma < 1$, where

$$\gamma_0 = \|\mathbf{T}_{ew}\|_\infty, \quad \gamma = \|\mathbf{T}_{ba}\|_\infty.$$

Indeed, we know from [4, Section 5] that a small value for $\frac{\gamma_0}{1-\gamma}$ will result in a small steady-state error.

We formulate a standard H^∞ problem for the control system shown in Figure 3, where $\tilde{w} = [v_1 \ v_2 \ w]^T$ and, in terms of Laplace transforms,

$$\begin{bmatrix} \tilde{z} \\ \tilde{y} \end{bmatrix} = \tilde{\mathbf{P}} \begin{bmatrix} \tilde{w} \\ u \end{bmatrix}, \qquad u = \mathbf{C}\,\tilde{y}.$$

Here, ξ and μ are nonzero parameters whose choice gives us more freedom in the design. The small parameter μ is introduced to satisfy a rank condition needed to make the H^∞ problem solvable and W_u is a weighting function whose value at infinity, $D_u = W_u(\infty) \neq 0$, is also needed for a rank condition. The problem formulation here is a slight improvement over the one in [4], where W_u was a constant. The fact that W_u is frequency-dependent allows us to choose it as a high-pass filter. This has the effect of reducing the controller gains at high frequencies. The realizations of W_u and W are:

$$W_u(s) = \left[\begin{array}{c|c} A_u & B_u \\ \hline C_u & D_u \end{array} \right], \quad W(s) = \left[\begin{array}{c|c} A_w & B_w \\ \hline C_w & 0 \end{array} \right]$$

and the generalized plant $\tilde{\mathbf{P}}$ can be represented as

$$\left[\begin{array}{ccc|ccc:c} A & 0 & 0 & 0 & 0 & B_1 & B_2 \\ B_w C_1 & A_w & 0 & B_w \xi & 0 & B_w D_{11} & B_w D_{12} \\ 0 & 0 & A_u & 0 & 0 & 0 & B_u \\ \hline 0 & C_w & 0 & 0 & 0 & 0 & 0 \\ 0 & 0 & C_u & 0 & 0 & 0 & D_u \\ \hdashline C_1 & 0 & 0 & \xi & 0 & D_{11} & D_{12} \\ C_2 & 0 & 0 & 0 & \mu I & D_{21} & D_{22} \end{array} \right]. \tag{2}$$

Using the μ-analysis toolbox from MATLAB$^{\text{TM}}$, we can find a controller $\mathbf{C}$ which nearly minimizes the H^∞-norm of the transfer matrix from $\tilde{w}$ to $\tilde{z}$, $\mathbf{T}_{\tilde{z}\tilde{w}} = \mathcal{F}_l(\tilde{\mathbf{P}}, \mathbf{C})$. However, this is *not* our final objective. We denote the central sub-optimal controller for a given norm of $\mathbf{T}_{\tilde{z}\tilde{w}}$ by

$$\mathbf{C}(s) = \left[\begin{array}{c|cc} A_c & B_{c1} & B_{c2} \\ \hline C_c & 0 & 0 \end{array} \right]$$

(note that its feedthrough matrix is equal to 0). After some manipulations, we obtain the realizations of $\mathbf{T}_{ew}$ and $\mathbf{T}_{ba}$, respectively, as

$$\mathbf{T}_{ew} = \left[\begin{array}{cc|c} A & B_2 C_c & B_1 \\ B_{c1} C_1 + B_{c2} C_2 & A_c + (B_{c1} D_{12} + B_{c2} D_{22}) C_c & B_{c1} D_{11} + B_{c2} D_{21} \\ \hline C_1 & D_{12} C_c & D_{11} \end{array} \right], \tag{3}$$

$$\mathbf{T}_{ba} = \left[\begin{array}{cc|cc} A & B_2 C_c & 0 & 0 \\ B_{c1} C_1 + B_{c2} C_2 & A_c + (B_{c1} D_{12} + B_{c2} D_{22}) C_c & 0 & B_{c1} \\ B_w C_1 & B_w D_{12} C_c & A_w & B_w \\ \hline 0 & 0 & C_w & 0 \end{array} \right]. \tag{4}$$

It is worth noting that the equations (2), (3) and (4) are valid for the general case, regardless of the dimension of the measurement vector, which here is the scalar i_c.

Using the parameters shown in Table 1, a nearly optimal controller, for which the Bode plots are shown in Figure 4, is obtained using $W_u(s) = \left[\begin{array}{c|c} -100000 & 1 \\ \hline -5000 & 0.05 \end{array} \right]$, $W(s) = \left[\begin{array}{c|c} -10000 & 10000 \\ \hline 1 & 0 \end{array} \right]$, $\xi = 14$ and $\mu = 0.5$ (these latter two were determined after an extensive search to minimize $\frac{\gamma_0}{1-\gamma}$ while keeping $\gamma < 1$). The Bode plots show that this controller is not realistic, because it has a very large bandwidth. In order to decrease the bandwidth, we do not minimize the H^∞-norm of $\mathcal{F}_l(\tilde{\mathbf{P}}, \mathbf{C})$ but find a central controller $\mathbf{C}$ such that $\left\| \mathcal{F}_l(\tilde{\mathbf{P}}, \mathbf{C}) \right\|_\infty$ is less than a given positive number (which is larger than the minimal value). The

Bode plots of an implementable controller are shown in Figure 5.

4 Simulation results

4.1 Nominal responses

Under the nominal conditions, the system obtains quite good performances. The output voltage and the tracking error are shown in Figure 6. The simulations are done in two different ways: with PWM block and without PWM block. In the first situation, the steady-state tracking error is about 0.5 V (peak), as shown in Figure 7(b), and in the second situation it is about 15 V (peak) (omitted because of page limit, but can be seen from Figure 6(b)).

A very large current surge (about half of the nominal load current), as shown in Figure 7(a), is applied to simulate the disturbance-rejection performance. The response is shown in Figure 7(b). As can be seen, the system has quite good capability to reject such a disturbance.

4.2 Responses to load changes

In this simulation, the load is changed to be a pure resistor of 6Ω. The output voltage and the tracking error are shown in Figure 8. The performance degradation cannot be observed from the figures.

4.3 Responses to grid distortions

Assume that the grid voltage is distorted as $V_g = 325 \sin \omega t + 32.5 \sin(3\omega t + \frac{\pi}{3}) + 81.25 \sin(5\omega t + \frac{\pi}{4})$, as shown in Figure 9(a). The static tracking error is less than 1 V (peak) as shown in Figure 9(b). Although the external grid is distorted so much, the local grid is very clean. (In order to make it clearer, the disturbance i_d is set to 0 and the PWM block is not activated in this simulation.)

5 Conclusions

This paper presents a possible circuit topology and the controller design for a grid-connected DC-AC power converter. The controller is designed using H^∞ control and repetitive control. Simulations show that the local grid voltage tracks the sinusoidal reference signal, even if there are nonlinear loads and the external grid is considerably distorted. When the load changes, the output voltage of the local grid tracks the reference voltage after a short transient.

References

[1]   Z. Chen and E. Spooner, "Grid power quality with variable speed wind turbines," *IEEE Trans. on Energy Conversion*, vol. 16, no. 2, pp. 148–154, 2001.

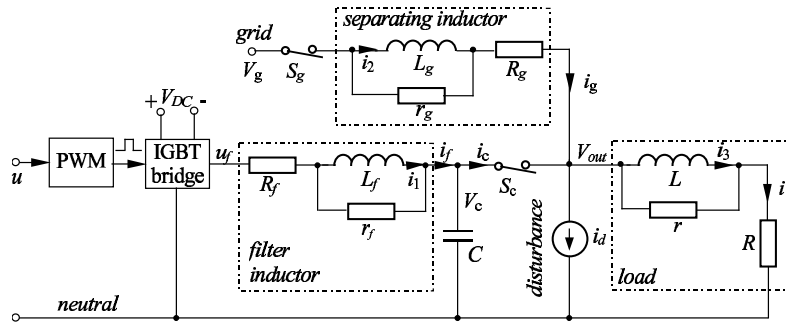[2]   M. Etezadi-Amoli and K. Choma, "Electrical performance characteristics of a new micro-turbine generator,"

Figure 1: The electrical diagram of the system

Table 1: Parameters of the system

parameter	value	parameter	value
R_f	0.053Ω	R_g	0.1Ω
L_f	1.3mH	L_g	0.3mH
r_f	30.5Ω	r_g	7Ω
R	5Ω	C	50μF
L	5mH	V_g	$230V, 50Hz$
r	500Ω	V_{DC}	$850V$
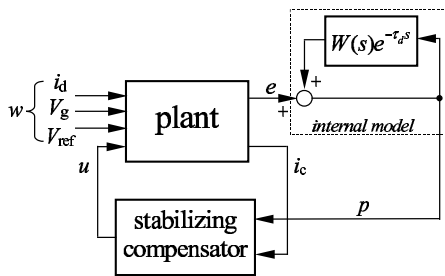
Figure 2: The robust repetitive control structure
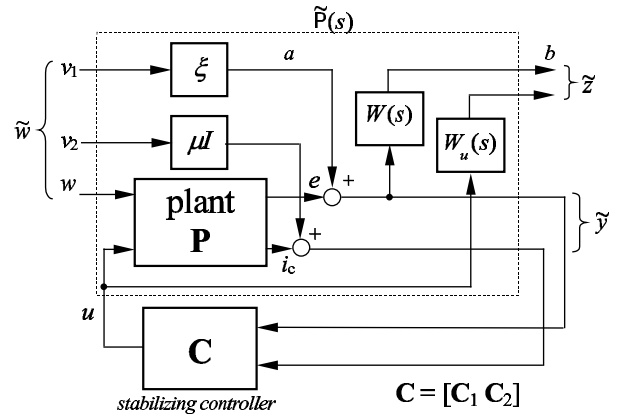
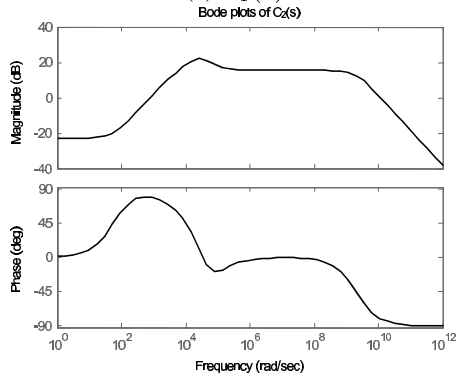**Figure 3:** Reformulation of the control problem

Trans. Industrial Electronics, vol. 48, no. 4, pp. 820–830, 2001.

[8] K. Zhou and J.C. Doyle, *Essentials of Robust Control*, Prentice-Hall, Upper Saddle River, N.J., 1997.

[9] M. Green and D.J.N. Limebeer, *Linear Robust Control*, Prentice-Hall, Englewood Cliffs, NJ, 1995.

in *IEEE Power Engineering Society Winter Meeting*, 2001, vol. 2, pp. 736–740.

[3] J.H.R. Enslin, M.S. Wolf, D.B. Snyman, and W. Swiegers, "Integrated photovoltaic maximum power point tracking converter," *IEEE Trans. Industrial Electronics*, vol. 44, no. 6, pp. 769 –773, 1997.

[4] G. Weiss and M. Hafele, "Repetitive control of MIMO systems using H_∞ design," *Automatica*, vol. 35, no. 7, pp. 1185–1199, 1999.

[5] Y. Yamamoto, "Learning control and related problems in infinite-dimensional systems," in *Essays on control: Perspectives in the theory and its applications*, H. Trentelman and J. Willems, Eds., pp. 191–222. Boston: Birkhäuser, 1993.

[6] K.L. Zhou, D. Wang, and K.-S. Low, "Periodic errors elimination in CVCF PWM DC/AC converter systems: repetitive control approach," *IEE Proc.Control Theory Appl.*, vol. 147, no. 6, pp. 694–700, 2000.

[7] K.L. Zhou and D. Wang, "Digital repetitive learning controller for three-phase CVCF PWM inverter," *IEEE*
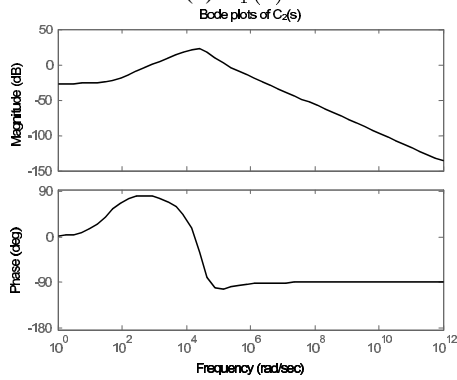
(a) $C_1(s)$

(b) $C_2(s)$

Figure 4: Bode plots of a nearly optimal controller. Note that it has a very large bandwidth, which is not realistic.
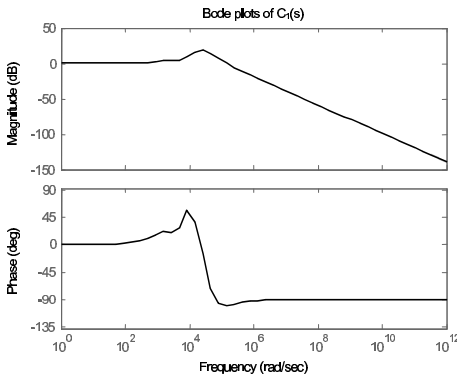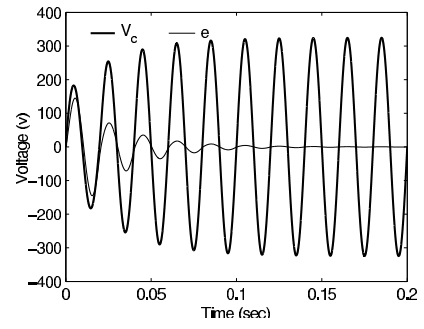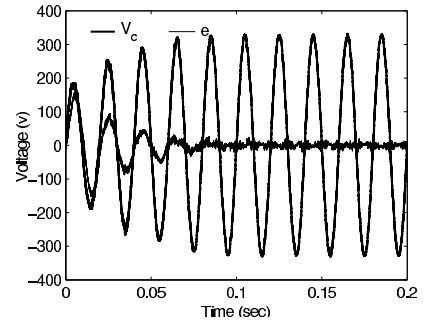

(a) $C_1(s)$

(b) $C_2(s)$

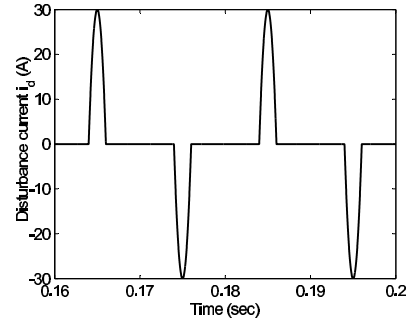**Figure 5:** Bode plots of a more realistic controller
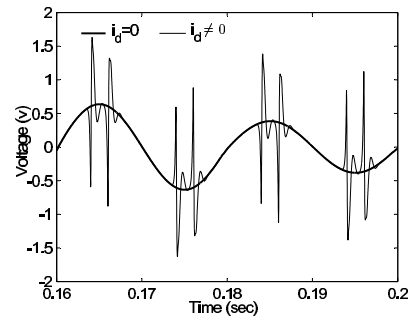

(a) Without PWM block

(b) With PWM block ($f_s = 10$kHz)

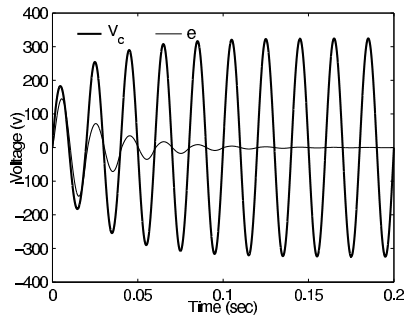**Figure 6:** The output voltage V_c and the tracking error e

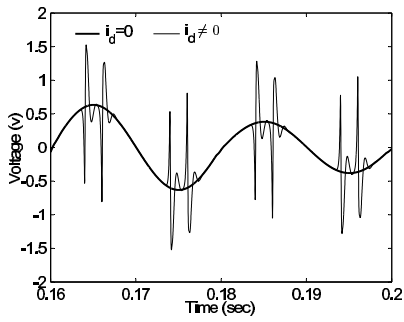(a) The disturbance current i_d

(b) The steady-state tracking error simulated without the PWM block

Figure 7: Disturbance responses for the nominal load (composed of an inductor and two resistors) shown in Fig. 1
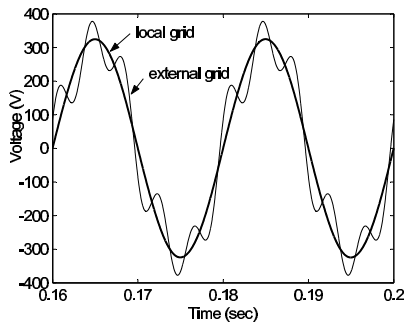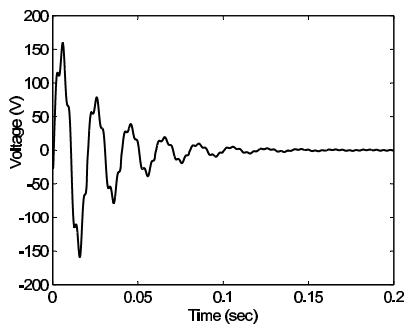
(a) The output voltage and the error

(b) The steady-state tracking error simulated without the
PWM block

Figure 8: The output voltage and the tracking error for a purely
resistive load of 6Ω

(a) The grid voltages

(b) The transient tracking error

Figure 9: The grid voltages and the tracking error